

Efficient twin aperture magnets for the future circular e^+/e^- collider

A. Milanese

CERN-The European Organization for Nuclear Research, CH-1211 Geneva, Switzerland

(Received 29 June 2016; published 2 November 2016)

We report preliminary designs for the arc dipoles and quadrupoles of the FCC-ee double-ring collider. After recalling cross sections and parameters of warm magnets used in previous large accelerators, we focus on twin aperture layouts, with a magnetic coupling between the gaps, which minimizes construction cost and reduces the electrical power required for operation. We also indicate how the designs presented may be further optimized so as to optimally address any further constraints related to beam physics, vacuum system, and electric power consumption.

DOI: 10.1103/PhysRevAccelBeams.19.112401

I. INTRODUCTION AND MAIN REQUIREMENTS

FCC-ee is the lepton collider within the Future Circular Collider (FCC) study. This machine is a double-ring synchrotron, colliding e^+/e^- with beam energies ranging from 40 to 175 GeV [1].

Several FODO lattices have been proposed for the arcs, with cell lengths of 50–60 m, separate function magnets and different integrated fields and gradients [2–3]. Table I lists the main requirements for the arc magnets, considering the highest beam energy. These values are still rather tentative, as the optics is evolving, though they allow drafting first cross sections for the magnets, useful for discussions on lattice, vacuum and power converters.

The natural choice, given the low fields, is to use resistive magnets. There are no particular requirements for the ramp rate, as a top up injector is in place.

The dipoles are kept as long as possible, to limit the synchrotron radiation losses. The integrated strengths of the focusing (QF) and defocusing (QD) quadrupoles are similar, though the QF is longer than the QD, again in an effort to limit the radiation emitted in the horizontal plane. As only two rf stations are foreseen, a tunability of the order of $\pm 1\%$ is desirable at high beam energy, to address the synchrotron radiation sawtooth.

As two separate rings with their corresponding magnets are needed, combining as much as possible the magnets of the two machines is interesting to decrease the number of units to manufacture, test, transport, install, maintain, and eventually remove (if needed to make room for FCC-hh). We consider here—besides a mechanical coupling—also a magnetic one: this brings in particular an advantage for the power consumption, which can be relevant in such a large machine.

Published by the American Physical Society under the terms of the Creative Commons Attribution 3.0 License. Further distribution of this work must maintain attribution to the author(s) and the published article's title, journal citation, and DOI.

II. HISTORICAL EXAMPLES

Examples of large synchrotrons with low field bending magnets are LEP and HERA (electron ring). Both machines are quite dated—first collisions took place in 1989 for LEP and in 1991 for HERA—though the technology of warm magnets is still very similar, so these cases can be instructive. In addition, we recall also the arc dipoles of the SLC (linear collider) at SLAC, and the twin aperture resistive quadrupoles of the LHC at CERN.

LEP was hosted in the 26.7 km tunnel which is currently used for the LHC. Although being an electron positron collider, it was designed as a single ring, circulating just a few bunch trains in opposite directions.

The LEP main dipoles [4–6] had a C layout, with steel-concrete cores and aluminum excitation bars, as in Fig. 1. A few parameters of interest here are recalled in Table II. The cores were 5.75 m long and they were assembled in blocks of six units. They contained only 27% of steel, the rest being filled with cement mortar. This dilution had the effect of amplifying the flux density in the iron with respect to the low values in the gap. However, early prototypes [7] had shown similar performances—even at low fields—using conventional full steel yokes. The choice was indeed dictated mostly by economic reasons and it required a careful construction, which included for example a systematic partial fissionation of the mortar after a 12 months aging period [8].

TABLE I. Main requirements of FCC-ee arc dipoles and quadrupoles, at 175 GeV per ring.

	Bend	QF	QD
Quantity (per ring)	6528	1460	1460
Field or gradient	60 mT	8.8 T/m	21.8 T/m
Length [m]	10.0	3.5	1.4
Total \int field or gradient	3917 Tm	44968 T	44560 T
Physical aperture [mm]	120 h \times 90 v	\varnothing 88	\varnothing 88

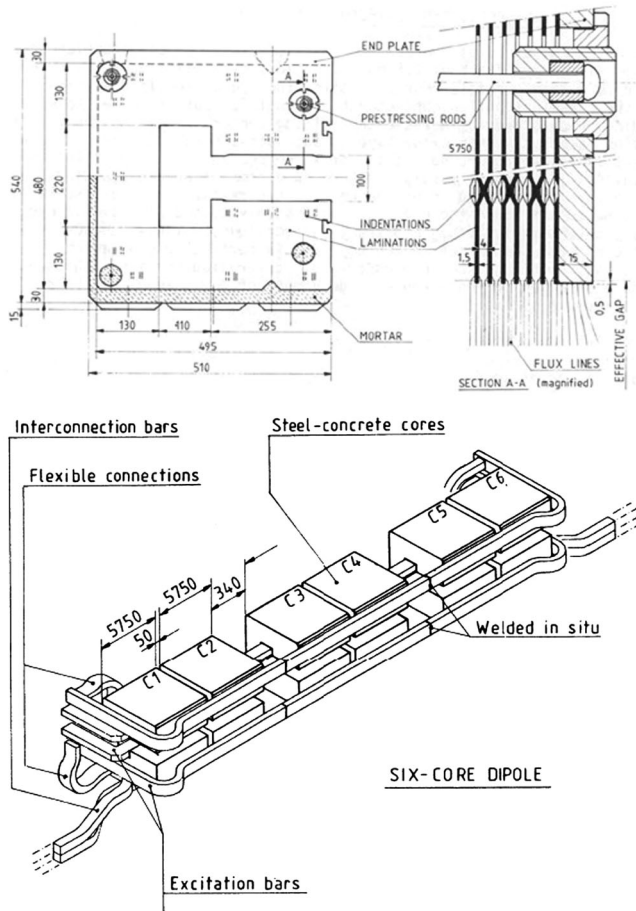


FIG. 1. Cross section and 3D sketch of the LEP dipoles.

The main LEP quadrupoles featured a classical design, with again aluminum conductor—either in the form of anodized strips or hollow cable. The regular lattice quadrupoles (MQ) were powered in two circuits, focusing and defocusing. In addition similar quadrupoles, though with a higher integrated gradient (MQA), were used in the dispersion suppressor and accelerating regions. The many circuits used to feed the MQA prompted a design with a lower operating current with respect to the MQ. Table III lists a few parameters of these magnets.

Both the LEP dipoles and quadrupoles were water cooled.

TABLE II. Main parameters of the LEP main bending magnets.

Number of magnets	488
Magnetic length [m]	35.01
Injection field @ 20 GeV [mT]	22
Field @ 100 GeV [mT]	108
Gap height [mm]	100
Pole width [mm]	255
Number of turns	2
Current @ 100 GeV [A]	4480
Current density @ 100 GeV [A/mm ²]	1.2

TABLE III. Main parameters of the LEP resistive quadrupoles.

	MQ	MQA
Number of magnets	488	256
Magnetic length [m]	1.60	2.00
Maximum gradient [T/m]	9.5	10.9
Aperture diameter [mm]	125	125
Number of turns per pole	29	58
Maximum current [A]	525	300
Current density @ maximum current [A/mm ²]	2.7	2.3

HERA was a 6.3 km electron proton collider, at DESY. While the proton ring was superconducting, the electron one was built with resistive technology [9]. A cross section of the bending magnets for the HERA electron ring is shown in Fig. 2, while their main parameters are recalled in Table IV. The yokes were built with compact C shaped 5 mm thick punched laminations, which were also welded to the support girder, to increase the stiffness.

The current was provided by water cooled aluminum busbars: one inside the C, two on the outside, to compensate with the return current the stray field. Differently from LEP, the opening of the C was in this case on the inside of the ring, with 90% of the emitted synchrotron radiation absorbed on the water cooled copper vacuum chamber. The field quality within ± 40 mm horizontally was homogeneous within 2×10^{-4} , once the $\pm 20 \times 10^{-4}$ of the (systematic) quadrupole component were subtracted [10].

The arc quadrupoles of the HERA electron ring were similar to the LEP ones, though with water cooled copper conductor instead of aluminum. Their main parameters are reported in Table V.

Table VI reports the power consumptions for the main magnets of LEP and HERA. For the dipoles, we list the power per meter, recomputed from the conductor cross section and the current; the connections have an important weight in the overall electrical budget and they have to be accounted for separately. For the quadrupoles, we list the power per magnet; in this case, the cable losses are less

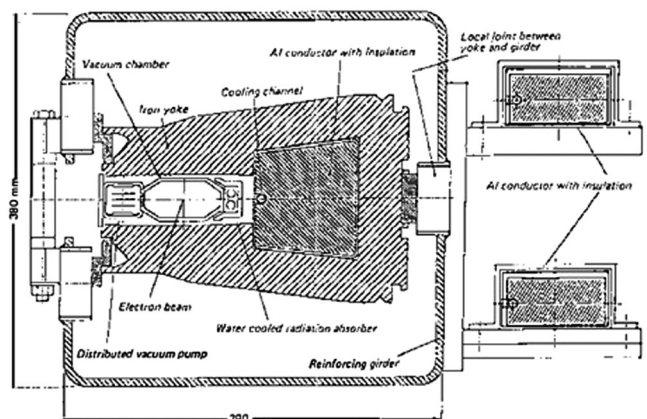


FIG. 2. Cross section of the HERA electron ring dipoles.

TABLE IV. Main parameters of the HERA resistive dipoles.

Number of magnets	416
Length [m]	9.19
Injection field @ 12 GeV [mT]	66
Field @ 30 GeV [mT]	164
Gap height [mm]	51
Pole width [mm]	154
Current @ 30 GeV [A]	6767
Current density @ 30 GeV [A/mm ²]	0.7

TABLE V. Main parameters of the HERA resistive quadrupoles.

Number of magnets	416
Length [m]	0.76
Gradient @ 30 GeV [T/m]	13.1
Aperture diameter [mm]	74
Number of turns per pole	20
Current @ 30 GeV [A]	358
Current density @ maximum current [A/mm ²]	2.4

TABLE VI. Power consumption of LEP and HERA (electron ring) main dipoles and quadrupoles.

Bending magnets, power per m (Al conductor)	
LEP @ 100 GeV [W/m]	550
HERA @ 30 GeV [W/m]	240
Main quadrupoles	
LEP MQ at maximum gradient (Al conductor) [kW]	17.9
LEP MQA at maximum gradient (Al conductor) [kW]	22.5
HERA @ 30 GeV (Cu conductor) [kW]	2.7
Totals (cable/busbar losses not included)	
Dipoles, LEP @ 100 GeV [MW]	9.4
Quadrupoles, LEP @ maximum gradient [MW]	14.5
Dipoles, HERA @ 30 GeV [MW]	0.9
Quadrupoles, HERA @ 30 GeV [MW]	1.1

significant. For both machines, the power to feed the quadrupoles is similar to that needed for the dipoles.

Another example of many resistive magnets for a lepton machine is the SLC at SLAC [11], with 940 2.5 m long magnets in its single pass arcs. The cross section is shown in Fig. 3. We do not report here in detail its parameters, as the aperture was rather small—only 16.4 mm of central vertical gap—and the dipole field was much higher than FCC-ee, namely 0.60 T at 50 GeV. These magnets had several features which are interesting in this context. The first is that they combined a dipole, quadrupole and sextupole field distribution, obtained with a peculiar three poles geometry. This allowed a very high filling factor of 96%. Then, the transverse size was kept compact, exploiting the minuscule dimensions of the beam; besides the small gap, the good field region was a mere

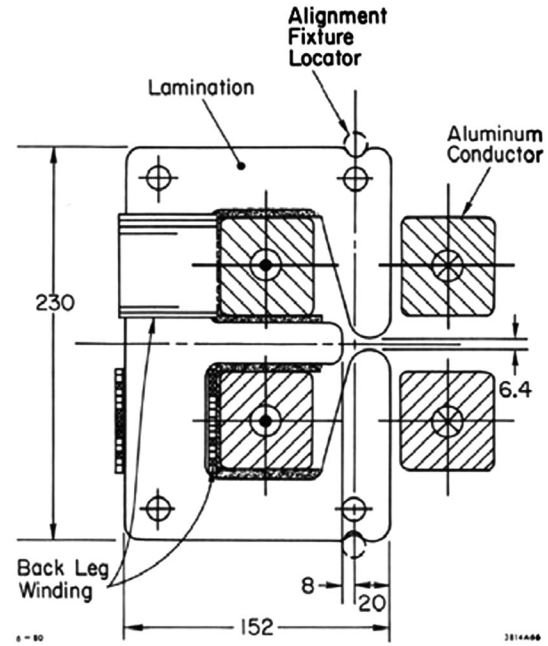


FIG. 3. Cross section of the SLC arc combined function dipoles.

± 4 mm (horizontally). Another feature was the strength tunability, of the order of $\pm 3\%$, provided through backleg windings, to follow in a tapered way the energy lost by synchrotron radiation. Finally—for a machine built in the U.S. at a similar time as LEP and HERA in Europe—the designers also opted for water cooled, low current density aluminum busbars, threaded along different cores.

To conclude this part, we recall the design of the MQW quadrupoles [12], installed in the LHC collimation regions. These are resistive magnets with water cooled copper coils, as shown in Fig. 4. A few parameters of interest are listed in Table VII. Although used in a high energy hadron machine, their pole tip field—0.8 T—is not much higher than the 0.5–0.7 T found in LEP and HERA. The interesting feature

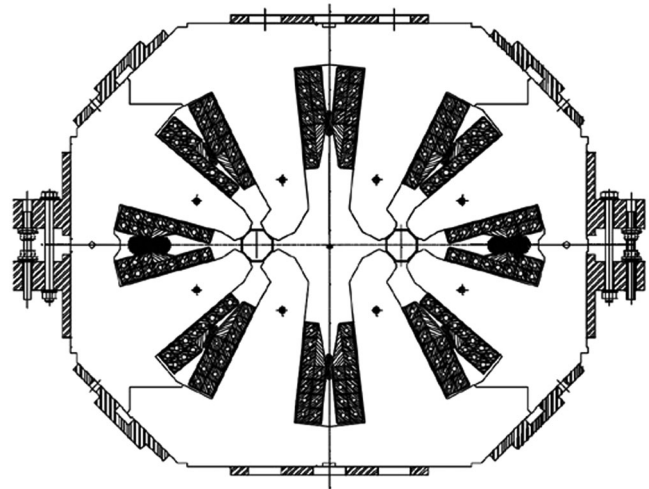


FIG. 4. Cross section of the MQW quadrupoles in the LHC.

TABLE VII. Main parameters of the MQW quadrupoles in the LHC.

Number of magnets	48
Iron length [m]	3.10
Nominal gradient [T/m]	35.0
Aperture diameter [mm]	46
Interbeam distance [mm]	224
Yoke width [mm]	976
Yoke height [mm]	706
Number of turns per pole	11
Nominal current [A]	710
Nominal current density [A/mm ²]	1.8–2.4
Nominal power (both apertures) [kW]	19.0

is their twin layout, with the two apertures hosted in the same yoke. This is an example of a purely mechanical coupling, as indeed there are the eight coils of two conventional quadrupoles, as if they were put side to side. The two apertures are basically independent and they can be powered with the same or opposite polarities.

III. FCC-EE MAIN BENDING MAGNETS

The aperture of the FCC-ee bending magnets (Table I) depends on the size of the vacuum chamber, which is in turn dictated by impedance and synchrotron radiation absorption [13], not directly by the beam size. The tentative vertical gap is similar to that of LEP.

On the other hand, the good field region can be more limited, exploiting the tiny dimensions of the beam: we set a few 10^{-4} of field homogeneity within ± 10 mm horizontally as a target, without counting a quadrupole term that—if systematic from magnet to magnet—can be dealt with, even if different at different dipole fields. No separate requirement is needed for the vertical good field region, as the beam is very flat, with an emittance ratio in the transverse planes of about 2000.

To provide parallel dipole fields for counterrotating beams, several layouts are possible, as shown for example in Fig. 5.

(a) A first option is to have completely separate dipoles, for example two C with the opening on the outside of the ring. The two independent powering circuits bring full flexibility, but also a factor of 2 for conductor mass and resistive power with respect to the other cases commented below.

(b) A modification of (a) is to use the return current of one dipole as excitation current for the other one. To get the parallel fields, the two C yokes need to be facing in opposite orientations, so for one beam the opening would be on the inside rather than the outside of the tunnel.

(c) A third option is a C dipole with a wide pole, hosting the two beams side by side. This layout can be interesting if a twin concept for the vacuum chamber can be exploited.

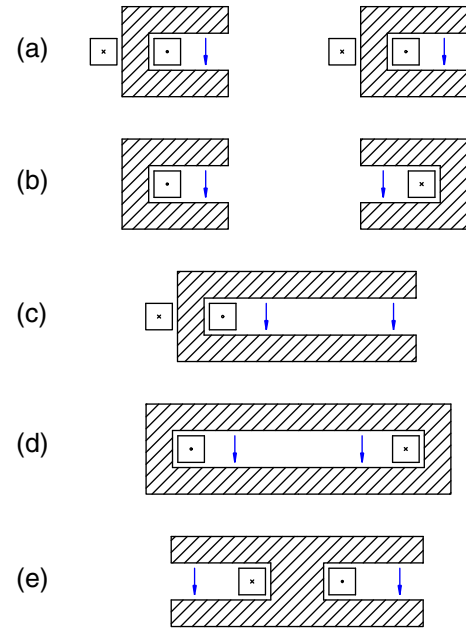


FIG. 5. Schematic layouts of twin dipoles arrangements: (a) two separate C magnets with independent powering circuits; (b) two C yokes, with a single shared excitation turn; (c) a single wide C dipole; (d) a wide O (or H, if needed) dipole; (e) an I layout. For (a) and (b), the separate magnets or yokes are not constrained to be side by side, and they can be mounted on a shared support structure.

(d) If a single wide dipole is considered, an O (or H, if needed for the Ampere turns) yoke can be another option. The potential advantages in terms of field homogeneity and compactness of the yoke would need to be evaluated, and weighted with the harder accessibility for the vacuum system.

(e) Finally, two parallel dipole fields can be achieved with what we refer to as an I design. This can be more compact than (d) when a large interbeam distance is needed; on the other hand, it requires separate vacuum chambers, which has been the baseline for the moment.

The two last arrangements can be thought of as limit cases of (b), with the two yokes touching on either side.

The optimal layout depends on several parameters, such as the vacuum chambers and synchrotron radiation absorbers (distributed or lumped), the interbeam distance, and possibly the strength and aperture of the quadrupoles—as a minimum physical separation of the two gaps is needed.

In the following we detail the I layout, which is rather unconventional: Fig. 6 shows the cross section while Table VIII lists the main parameters. Many of the considerations apply to the other options¹ sketched in Fig. 5.

¹Layout (a) with two separate magnets is more of an exception, for its double power consumption and conductor mass with respect to the others.

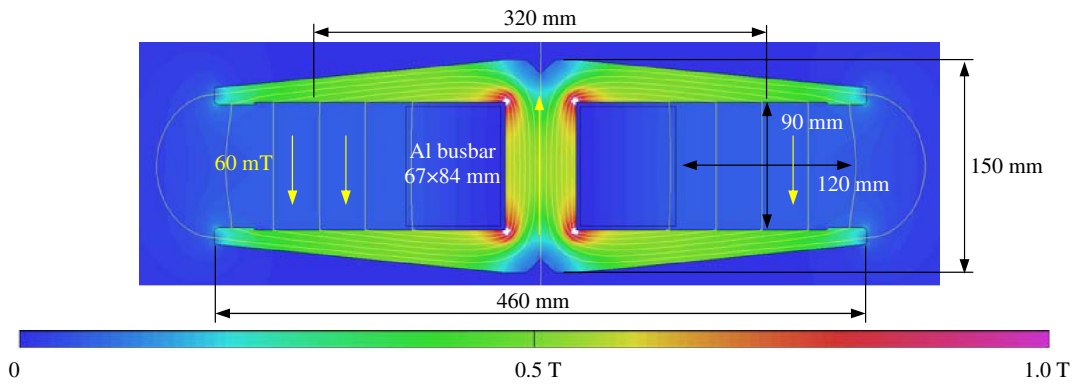


FIG. 6. First cross section of FCC-ee bending magnets with an I layout (field levels for 175 GeV).

As for the large machines recalled above, we also propose aluminum busbars as conductors. Avoiding multi-turns coils—which is feasible since only a few kA at most of current are needed—lowers the capital cost, bringing at the same time a few other advantages, like the absence of interturn insulation (a possible weak point, especially under radiation load) and the possibility of threading across several units, to increase the arc filling factor keeping the length of the yokes compatible with transport and handling limits. Indeed having a busbar in the midplane instead of a conventional coil could be exploited to handle any residual synchrotron radiation, in particular for the aperture facing on the inside of the ring. Proper bypasses in correspondence of the other magnets become important. These are a significant source of power dissipation, in the form of cable (or better, busbar) losses. Then, in order to limit magnetic perturbations, the busbars—when crossing short or long straight sections—need to be screened, and/or brought near to each other. From the economical viewpoint, for a cross section with the same electrical resistance, the cost of the raw material (in early 2016) is about a factor 6.5 lower for Al compared to Cu, while being 2 times lighter. The current density is quite low even at the highest field; still the capital investment related to the conductor remains rather moderate. Moreover, since the radiation activation of Al is expected to be lower than Cu, the raw material can be more conveniently recycled after exploitation of the machine, when this has to be dismantled to make room

for a high energy hadron collider. We consider direct water cooling (the relevant duct is not shown in Fig. 6) as it is likely more convenient than adding the heat load to the tunnel ventilation, especially if cooling water is used anyway for the vacuum chambers and absorbers. This choice was in fact pursued for both LEP and HERA.

Separate windings on the individual halves (not shown in Fig. 6) can be added, for a few percent tuning capability, to scale the strength according to the synchrotron radiation lost along the arcs at high beam energy, and possibly to act as horizontal correctors.

The interbeam distance of 320 mm is not a constraint coming from the optics, but only a proposal based on the I dipole layout, its pole width and conductor size. For comparison, this distance in the LHC arcs is 194 mm.

Table IX reports the 2D allowed multipoles, simulated using a nonlinear BH characteristics of a typical electrical steel. Though the layout is not fully optimized (for example, the sensitivity of the field quality with respect to the position of the busbars needs to be assessed), still, profiting from the small reference radius, all harmonics are already below 10^{-4} , except b_2 , which can be handled separately. The sextupole and higher order terms remain the same at the two excitation levels, with only the gradient exhibiting a weak dependence with the field. This implies that a change in iron permeability impacts mainly the quadrupole component only. Actually, the pole profile—straight in Fig. 6—can be tweaked to add (or control) a quadrupole term. Such an option is shown in

TABLE VIII. Main parameters of the FCC-ee I dipoles.

Field @ 175 GeV [mT]	60
Gap height [mm]	90
Overall width/height [mm]	460/150
Number of turns	1
Current @ 175 GeV [A]	4440
Current density @ 175 GeV [A/mm ²]	0.8
Mass of steel per m [kg/m]	190
Mass of aluminum per m [kg/m]	30
Resistance per m [$\mu\Omega$ /m]	9.4
Power per m @ 175 GeV [W/m]	190

TABLE IX. Simulated 2D field homogeneity for the twin dipole of Fig. 6; the allowed harmonics are at 10 mm radius.

Beam energy [GeV]	45	175
B_1 [mT]	15	60
b_2 [10^{-4}]	-6.0	-4.2
b_3 [10^{-4}]	-0.3	-0.4
b_4 [10^{-4}]	-0.5	-0.5
b_5 [10^{-4}]	-0.1	-0.1
b_6 [10^{-4}]	0.0	0.0

Fig. 8, using an inclined circular arc at the pole, with a slope of 4 deg. This value is rather arbitrary, and higher gradients can be obtained; for example, in the PS main magnets at CERN the equivalent central pole slope is 12 deg. It is possible to have also a sextupole term, such as for example in the SLC, in synchrotron light boosters [14], and the CERN ISR [15]. Bending magnets with embedded quadrupole and sextupole terms, together with quadrupole magnets with a quadratic term, are expected to beneficially increase the arc filling factor.

The lowest dipole field is 15 mT, not far from the 22 mT of LEP at injection. Back then, the field was amplified to 81 mT in the iron at the pole, thanks to the heavy dilution. However, undiluted prototypes had been successfully tested down to 17 mT [7], with only the (unwanted) quadrupole term affected. Then, also this design features a field amplification in the iron—likely beneficial at low excitations—which is achieved through the wide and thin poles: 60 mT in the gap corresponds on average to 0.5 T along a central flux line. Finally, the operation of FCC-ee involves a top up injection, differently from LEP, which was ramped. Therefore, to run at different but constant beam energies, if the magnets were to be powered at a higher excitation first, then the remanent field could be addressed through conditioning precycles, if needed.

Engineering of the actual yoke would need to consider at once economic and manufacturing factors, for the thousands of units to be produced. An option could be to stack punched thick laminations, 5–6 mm (as in HERA or LHC) or more, up to 12 mm (which is what is obtained in hot rolling of electrical steel). Alternatively, the same techniques used to make construction steel I beams could be envisaged, like rolling the final section, or welding separate plates—possibly adding a machining stage of the poles. Furthermore, the need of a separate support structure adding stiffness would need to be evaluated. This I layout is symmetric to torsion with respect to a C geometry; the longitudinal bending due to self-weight could be compensated at manufacturing, and it might anyway be not critical for field quality. The magnetic force between the poles remains rather low: for the highest field, it is equivalent—per aperture—to the weight of the Al busbar.

To have an idea of the resistive voltage (as the inductive component is less of a concern here), we use the resistance per unit meter and we consider a 100 km (double) circuit, thus taking the same busbar cross section for the bypasses. Even for this (extreme) case with no sectorization of powering, we end up with 4.2 kV of resistive voltage at the highest excitation current, that is, ± 2.1 kV to ground. This value will likely be lower, once an adequate

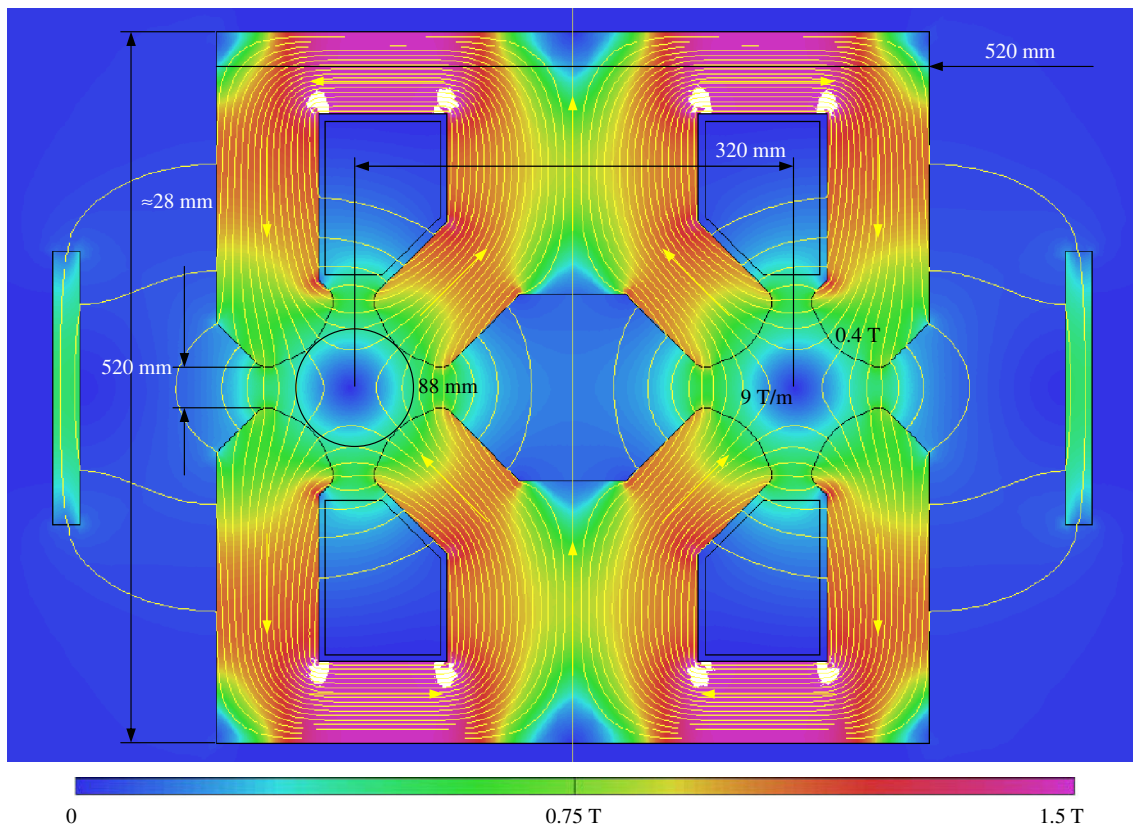


FIG. 7. First cross section of FCC-ee twin quadrupoles; the geometry is to scale with the twin dipole of Fig. 6 (field levels for 175 GeV).

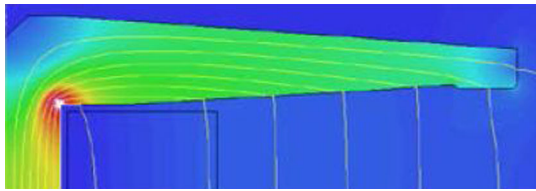


FIG. 8. Example of pole profile (1/4 of cross section shown) for a combined function magnet; in this case, the central slope is 4 deg, yielding a gradient of 86 mT/m for a field of 60 mT. The colorbar follows the same scale of Fig. 6.

sectorization of powering is put in place. However, we foresee no special requirements on the electric insulation, which could thus be of a conventional type; an inorganic coating, for example of alumina, could possibly be used both for cost effectiveness and radiation resistance (if the busbars absorb some remaining radiation on the midplane). Finally, also to estimate the total power we take a 100 km circuit, as to include the cable losses. This results in 18.6 MW at a beam energy of 175 GeV.

IV. FCC-EE MAIN QUADRUPOLES

The focusing and defocusing quadrupoles—as for the requirements of Table I—differ in lengths and gradients, but they are basically equivalent for integrated strengths, with 30.8 T for QF and 30.5 T for QD. We propose here to lengthen the QD, so that the two magnets become the same, and magnetically coupled twin designs can be explored.² This extra length would need an iteration with the lattice design, to provide a consistent cell layout.

The pole tip field at the highest beam energy is then 0.39 T, lower than the 0.48 T of HERA or the 0.59 T of the LEP MQ. Also in this case the natural choice is to use warm magnets. Separate units would be a trivial choice, with likely narrow figure-of-8 yokes, depending on the interbeam distance. These two quadrupoles could be mounted side by side on the same support structure. At the limit, a solution based on a single shared yoke—similar to the MQW at LHC of Fig. 4—can be envisaged. This option allows independent strengths in the two apertures, with are coupled only mechanically. This kind of design is not further pursued here.

On the other hand, in Fig. 7 we propose a twin quadrupole design. In this cross section, there are eight poles—four for each aperture—but only two (simple racetrack) coils in total. The Ampere turns are in fact wound around the central shared legs: the flux thus generated then equally distributes in the two gaps. This yields a full magnetic coupling of the two apertures, which exhibit a focusing/defocusing polarity—as seen by the beams. This is a constraint, but it brings a net gain of 50%

²This also assumes that the physical locations of the quadrupoles in the two rings are the same.

TABLE X. Main parameters of the FCC-ee twin quadrupoles.

Gradient @175 GeV [T/m]	8.8
Aperture diameter [mm]	88
Length [m]	3.5
Interbeam distance [mm]	320
Yoke height [mm]	520
Yoke width (with/without shields) [mm]	520/760
Number of coils	2
Ampere turns per coil @ 175 GeV [A]	13750
Current density @ 175 GeV [A/mm ²]	2.3
Power per twin magnet @ 175 GeV [kW]	8.7

for the total Ampere turns, corresponding also to 50% dissipated power (at equal current density) with respect to a design like MQW. For comparison, the main quadrupoles in the LHC (superconducting) have independent powering circuits, though they are run with an F/D polarity—from the beams' perspective—with typically only a 5% difference in gradient.

This design is compatible with individual trims to be mounted on the separate apertures, for example on the outer legs, which can be used to tune the strengths in the two gaps. Another combination of trims could even provide some horizontal dipole term, so to add a (weak) vertical corrector on top of the quadrupoles.

The yoke geometry is asymmetric, still good field quality is possible by properly designing the pole tips—in 2D and 3D. If needed, weak systematic components could be dealt with by a few lumped correction magnets. The midplane is open, to avoid a magnetic short circuit; there is also a rather generous vertical opening between adjacent poles: both features could be exploited by the vacuum system. To control the stray field on the midplane, we add iron shields on the sides.

The aperture fulfills the requirement of Table I; the interbeam distance is kept the same as the I dipole of Fig. 6. The central leg could actually be hollowed, or made thinner, were a reduction of the interbeam distance possible.

Table X lists the main parameters of the twin quadrupoles. The Ampere turns are given per coil rather than per pole, due to peculiarity of the design. The current density is computed from the area shown in Fig. 7 taking a conductor filling factor—to include insulation and cooling ducts—equal to 70%. The resulting 2.3 A/mm² (at 175 GeV) is similar to that of HERA and LEP and it limits the power consumption, with respect to using smaller coils with a higher current density. This power estimate is given per magnet, considering also the coil ends, and taking Cu as conductor. Using Al instead and keeping the same coil cross section would involve a power increase of 54%. The total power (without cable losses, which are less important than for the dipoles) is estimated at 25.4 MW.

The actual resistance per magnet depends on the coil design and in particular on the number of turns.

This involves an overall optimization, including cables and power converters.

The 2D gradient could be increased to shorten the magnet length, if needed. The yoke would become larger, especially in the top/bottom return legs, and in the pole legs. Keeping the same coil cross section, if the 2D gradient is multiplied by k , while the length is shortened by k , the power would increase by the same factor k . To compensate for this, the coil could grow larger, to lower the current density. On the other hand, a decrease of the aperture diameter is accompanied by a quadratic reduction of the power, if the current density is kept the same.

The mechanical construction could be achieved by using stamped laminations. Several options are possible to split the yoke to install the coils, for example six laminations (two different types), or four pieces (again, two different types). The top/bottom halves could be held together by a nonmagnetic spacer, such as a continuous wide bar in the center.

Finally, other layouts are also possible. We presented for example in [16] a symmetric twin quadrupole design, with a similar full magnetic coupling between the apertures, but only a 25% saving (instead of 50%) for the power consumption.

V. CONCLUSIONS

We presented first twin aperture cross sections for the main FCC-ee dipoles and quadrupoles. These resistive magnets feature a full magnetic coupling between the two apertures, which brings a 50% saving in power consumption with respect to separate units. The implications to the optics have to be evaluated, possibly considering trim windings for tunability. Thanks to these innovative layouts, at the highest beam energy of 175 GeV, the total power for the magnets can be kept below 20 MW for the dipoles and below 30 MW for the quadrupoles.

For the bending magnets, we highlighted the possibility of combining a quadrupole (and even sextupole) term in the pole design, as a means to further increase the arc filling factor.

ACKNOWLEDGMENTS

We acknowledge a discussion with Philippe Lebrun about topological arrangements of yoke/coils in dipoles, leading to the I design. We thank Davide Tommasini for continued support for this activity, and for suggesting shields for the open midplane twin quadrupole.

- [1] J. Wenninger *et al.*, CERN EDMS Report No. 1346081, 2014.
- [2] K. Oide *et al.*, Design of beam optics for the FCC-ee collider ring, in *Proceedings of the International Particle Accelerator Conference, Busan, Korea, 2016*, THPOR022, doi:[10.18429/JACoW-IPAC2016-THPOR022](https://doi.org/10.18429/JACoW-IPAC2016-THPOR022).
- [3] B. Haerer *et al.*, First considerations on beam optics and lattice design for the future electron-positron collider FCC-ee, in *Proceedings of the International Particle Accelerator Conference, Richmond, 2015*, TUPTY059, <http://accelconf.web.cern.ch/AccelConf/IPAC2015/papers/tupty059.pdf>.
- [4] CERN Report No. CERN-LEP-84-01, 1984, <https://cds.cern.ch/record/102083?ln=en>.
- [5] L. Resegotti, The LEP magnet system, *J. Phys. (Paris), Colloq.* **45**, C1-233 (1984).
- [6] M. Giesch and J. P. Gourber, The bending magnet system of LEP, in *11th International Conference on Magnet Technology, Tsukuba, 1989*, http://link.springer.com/chapter/10.1007%2F978-94-009-0769-0_21.
- [7] J. P. Gourber and L. Resegotti, Implication of the low field levels in the LEP magnets, *IEEE Trans. Nucl. Sci.* **26**, 3185 (1979).
- [8] J. Billan, J. P. Gourber, K. N. Henrichsen, H. Laeger, and L. Resegotti, Influence of mortar-induced stresses on the magnetic characteristics of the LEP dipole cores, *IEEE Trans. Magn.* **24**, 843 (1988).
- [9] G.-A. Voss and B. H. Wiik, The electron-proton collider HERA, *Annu. Rev. Nucl. Part. Sci.* **44**, 413 (1994).
- [10] H. Kaiser, DESY Report No. DESY M-86-10, 1986, http://inspirehep.net/record/939367/files/HEACC86_II_294-296.pdf.
- [11] G. E. Fischer *et al.*, SLC arc transport system—magnet design and construction, *IEEE Trans. Nucl. Sci.* **32**, 5 (1985).
- [12] G. de Rijk, S. Bidon, E. Boter, G. S. Clark, O. Hans, M. Racine, and A. Salinas, Construction and measurement of the pre-series twin aperture resistive quadrupole magnet for the LHC beam cleaning insertions, *IEEE Trans. Appl. Supercond.* **12**, 55 (2002).
- [13] F. Zimmermann, K. Oide, and R. Kersevan (personal communication).
- [14] G. Benedetti *et al.*, Modeling results for the ALBA booster, in *Proceedings of the 2nd International Particle Accelerator Conference, San Sebastián, Spain (EPS-AG, Spain, 2011)*, WEPC025, <http://epaper.kek.jp/IPAC2011/papers/wepc025.pdf>.
- [15] E. Keil and L. Resegotti, Characteristic features of the CERN ISR magnet system, in *5th International Conference on High-Energy Accelerators, Frascati, 1965*, <https://cds.cern.ch/record/2060344?ln=en>.
- [16] A. Milanese, Thoughts about the main FCC-ee warm magnets, slides presented during the FCC week in Rome, Italy, 2016, <https://indico.cern.ch/event/438866/contributions/1084993/>.